

Weightbearing Computed Tomography of the Foot and Ankle: Emerging Technology Topical Review

Foot & Ankle International®
2018, Vol. 39(3) 376–386
© The Author(s) 2017
Reprints and permissions:
sagepub.com/journalsPermissions.nav
DOI: 10.1177/1071100717740330
journals.sagepub.com/home/fai

Alexej Barg, MD¹, Travis Bailey, MD¹, Martinus Richter, MD, PhD², Cesar de Cesar Netto, MD³, François Lintz, MD, FEBOT⁴, Arne Burssens, MD⁵, Phinit Phisitkul, MD⁶, Christopher J. Hanrahan, MD, PhD⁷, and Charles L. Saltzman, MD¹

Abstract

In the last decade, cone-beam computed tomography technology with improved designs allowing flexible gantry movements has allowed both supine and standing weight-bearing imaging of the lower extremity. There is an increasing amount of literature describing the use of weightbearing computed tomography in patients with foot and ankle disorders. To date, there is no review article summarizing this imaging modality in the foot and ankle. Therefore, we performed a systematic literature review of relevant clinical studies targeting the use of weightbearing computed tomography in diagnosis of patients with foot and ankle disorders. Furthermore, this review aims to offer insight to those with interest in considering possible future research opportunities with use of this technology.

Level of Evidence: Level V, expert opinion.

Keywords: weightbearing computed tomography, imaging of the foot and ankle

Background

Imaging remains highly valuable in diagnosing, treating, and assessing outcomes in patients with disorders of the foot and ankle. Available modalities include conventional radiographs, fluoroscopy, computed tomography (CT), scintigraphy, single-photon emission CT (SPECT-CT), magnetic resonance imaging (MRI), and ultrasonography. Most diagnostic imaging workups start with conventional weightbearing radiographs because pathologies such as subtle arch collapse and loss of cartilage are more reliably identified with weightbearing. Further imaging may be required for better assessment of the underlying pathology as well as to guide treatment planning. The choice of the best imaging modality is usually based on several factors that include (1) reliability with regard to the diagnosis under consideration; (2) local availability; (3) patient concerns, such as cost, convenience, and discomfort; (4) safety risks, including radiation dose (Table 1) and contrast sensitivity; and (5) cost.²²

CT technology is commonly used to evaluate skeletal pathology. Modern multidetector CT technology provides high-resolution thin-slice images that can be obtained in any plane, providing excellent visualization of fractures, degenerative changes, osseous union at a site of arthrodesis,

internal fixation of fractures, or osteotomies.²² One major limitation of conventional CT has been the inability to obtain weightbearing images. Without weightbearing during CT assessment, true alignment may not be fully appreciated. Pathology such as impingement, joint space narrowing,

¹Department of Orthopaedics, University of Utah, Salt Lake City, UT, USA

²Department for Foot and Ankle Surgery Nuremberg and Rummelsberg, Schwarzenbruck, Germany

³Department of Orthopaedics, University of Alabama at Birmingham, Birmingham, AL, USA

⁴Foot and Ankle Surgery Department, Clinique de l'Union, Saint-Jean, Toulouse, France

⁵Department of Orthopaedic Surgery, Ghent University Hospital, Ghent, Belgium

⁶Department of Orthopaedic and Rehabilitation, University of Iowa, Iowa City, IA, USA

⁷Department of Radiology and Imaging Sciences, Musculoskeletal Imaging, University of Utah, Salt Lake City, UT, USA

Corresponding Authors:

Alexej Barg, MD, Department of Orthopaedics, University of Utah, 590 Wakara Way, Salt Lake City, UT 84108, USA.

Email: alexej.barg@hsc.utah.edu

Charles L. Saltzman, MD, Department of Orthopaedics, University of Utah, 590 Wakara Way, Salt Lake City, UT 84108, USA.

Email: charles.saltzman@hsc.utah.edu

Table 1. Typical Effective Radiation Dose.^{22,25}

Characteristic	Dose, mSv
Average US background radiation/	3.0
Single transatlantic flight	0.04
Radiograph: chest (p.a.)	0.02
Radiograph: foot (single exposure)	0.001
Conventional computed tomography: pelvis	15
Conventional computed tomography: ankle	0.07
Cone-beam weightbearing computed tomography: foot/ankle	0.01-0.03
Isotope (tc-99m-MDP) bone scan	6.3

Abbreviations: MDP, methylene diphosphonate; mSv, millisievert; p.a., posteroanterior.

and malalignment that may be apparent only with load may also go undiagnosed.¹

The idea of visualizing the relative alignment of the bones of the foot and ankle with a weightbearing CT (WtBCT) imaging is not new. Several investigators have developed methods to simulate weightbearing using custom-made loading frames to assess foot and ankle pathologies (Table 2). The limitations of simulated weightbearing conditions have been well articulated by these authors. First, only partial weightbearing can be applied, so the observed deformities or pathologies are potentially underestimated compared to normal standing.^{1,2,9,11,19,24} Second, the loading devices are generally passive, applying external loads without the muscle forces active when standing.^{8,14,15}

In the past decade, cone-beam CT technology has helped with both supine and standing weightbearing imaging of the lower extremity due to improved designs with flexible gantry movements.^{4,29} This imaging technology has several advantages, including the ability to obtain images with the patient standing, high-contrast resolution and spatial resolution, fast image acquisition time, decreased radiation, a relatively small scanner size with portable design, and generally less capitalization cost than conventional CT scan technology.^{4,29}

The purpose of this report is to summarize the early literature investigating weightbearing CT. To do so, we performed a literature review of relevant clinical studies targeting the use of weightbearing CT in patients with foot and ankle disorders.

Studies on Normal Controls

Colin et al⁶ performed WtBCT in 59 patients without any history of hindfoot or ankle pathology to describe the subtalar joint configuration. The shape of the posterior facet and the subtalar vertical angle were measured in 3 different coronal planes (center of the subtalar joint, 5 mm anterior, and 5 mm posterior to the center). In this patient cohort, the

posterior facet was concave in 88% of feet and flat in the remaining 12%. In the middle coronal plane, the posterior facet was oriented in valgus in 90% and in varus in 10% of cases. However, substantial intraindividual differences in the patients were observed, with the subtalar vertical angle increasing in valgus when the measurement was performed more posteriorly.⁶

Meanwhile, Lepojärvi et al²¹ used WtBCT to investigate the normal anatomy and rotational dynamics of the distal tibiofibular joint under physiological conditions in a cross-sectional study including 32 asymptomatic patients. Imaging acquisition was performed in 3 different positions of the ankle: neutral, internal, and external rotation. Measured parameters included sagittal translation of the fibula, anterior and posterior widths of the distal tibiofibular syndesmosis, tibiofibular clear space, and rotation of the fibula. In patients with the ankle in neutral position, the fibula was located anteriorly in the tibial incisura in 88% of all measurements. During ankle rotation, the mean anteroposterior motion was 1.5 mm and the mean rotation of the fibula was 3 degrees.²¹

In another study, Lepojärvi et al²⁰ performed WtBCT in the same patient cohort to assess the rotational dynamics of the talus. The rotation of the talus, medial clear space, anterior and posterior widths of the tibiotalar joint, translation of the talus, and talar tilt were measured. When the ankle was rotated with a moment of 30 Nm, a talus rotation of 10 degrees without substantial widening of the medial clear space was observed.²⁰

Studies on Pathologic Conditions

In total, 8 studies were reviewed (Table 3). All were published between 2013 and 2017 with 4 prospective and 4 retrospective studies. All studies but 1 were single center in design. For the included investigations, the level of evidence ranged from II to IV. There was 1 level II study, 5 level III studies, and 2 level IV studies.

Collan et al⁷ used CT in weightbearing and nonweightbearing conditions in 10 patients with hallux valgus and 5 asymptomatic controls to assess the alignment of the first metatarsal bone. There were significant differences between weightbearing and nonweightbearing measurements of first metatarsal alignment in patients with hallux valgus deformity. For instance, the 3D hallux valgus angle was 35 ± 3 degrees in the weightbearing vs 46 ± 5 degrees in the nonweightbearing conditions.⁷

Hirschmann et al¹² performed a prospective study comparing CT of the hindfoot in the supine nonweightbearing position vs the upright weightbearing position. Hindfoot alignment was independently measured by 2 musculoskeletal radiologists in 22 patients with different indications for CT assessment, including osteoarthritis of the hindfoot ($n = 8$), osteochondral defects of the talus ($n = 6$), evaluation of

Table 2. Literature Review Addressing the Use of Simulated Weightbearing Computed Tomography in Patients With Foot and Ankle Disorders.

Study	Patients	Study Objectives	Methods	Findings
Ananthakrisnan et al, 1999 ¹	<ul style="list-style-type: none"> • 4 healthy controls • 8 patients with flatfoot deformity and rupture of PTT 	3D position of the talocalcaneal joint in patients with flatfoot deformity	75-N axial force with a custom loading frame in supine position	Patients with PTTD had decreased contact surface in the talocalcaneal joint
Apostle et al, 2014 ²	<ul style="list-style-type: none"> • 20 healthy controls • 20 patients with peritalar subluxation 	Morphology of the subtalar joint axis	75-N axial force with a custom loading frame in supine position	Subtalar joint axis orientation was more valgus in patients with peritalar subluxation
Ferri et al, 2008 ⁹	<ul style="list-style-type: none"> • 8 healthy controls • 15 patients with symptomatic flatfoot deformity 	Forefoot and hindfoot alignment	Special loading device with load of 50% of body weight	Forefoot arch angle 29% lower in flatfeet during nonweightbearing and 52% lower during weightbearing
Geng et al, 2015 ¹⁰	<ul style="list-style-type: none"> • 10 healthy controls • 10 patients with HV deformity 	Mobility of the first TMT joint	Special frame with full weightbearing in supine position	First TMT joint more dorsiflexed and more supinated in HV
Greisberg et al, 2003 ¹¹	<ul style="list-style-type: none"> • 37 patients with flatfoot deformity 	Assessment of deformity and degenerative changes	75-N axial force with a custom loading frame in supine position	<ul style="list-style-type: none"> • Mean TN angle -1 degree (10 to -34 degrees) • Mean naviculocuneiform angle -15 degrees (-1 to -30 degrees) • Average TMT subluxation 9% (0%-20%)
Katsui et al, 2016 ¹³	<ul style="list-style-type: none"> • 142 patients with HV deformity (269 feet) 	Alignment of the tibial sesamoid	Special frame with one-third of patient's weight loading	<ul style="list-style-type: none"> • Sesamoid position: grade 1 (tibial sesamoid medial to axis of first metatarsal), 34 feet; grade 2 (tibial sesamoid below the axis of the first metatarsal), 116 feet; grade 3 (tibial sesamoid lateral to axis of the first metatarsal), 119 feet
Kido et al, 2011 ¹⁴	<ul style="list-style-type: none"> • 21 healthy controls • 21 patients with flatfoot deformity 	Bone rotation of hindfoot joints	A custom foot loading device with 99.4% ± 11.6% of the body weight	Patients with flatfoot deformity: talus, 1.7 degrees more plantarflexed; navicular, 2.3 degrees more everted; calcaneus, 1.1 degrees more dorsiflexed and 1.7 degrees more everted
Kido et al, 2013 ¹⁵	<ul style="list-style-type: none"> • 20 healthy controls • 24 patients with flatfoot deformity 	Bone rotation of each joint in the medial longitudinal arch	Special frame with full weightbearing in supine position	Patients with flatfoot deformity: first metatarsal more dorsiflexed, navicular and calcaneus more everted, and TN joint more rotated
Kim et al, 2015 ¹⁶	<ul style="list-style-type: none"> • 138 patients (166 feet) with HV deformity • 19 healthy controls (19 feet) 	First metatarsal pronation and sesamoid position	Special frame with half of full weightbearing in supine position	Significant difference in α angle with 21.9 degrees (HV group) vs 13.8 degrees (control group)
Kimura et al, 2017 ¹⁷	<ul style="list-style-type: none"> • 10 patients with HV deformity • 10 healthy controls 	3D mobility of the first ray	Special frame with full weightbearing in supine position	Patients with HV deformity: TN and first TMT joints more dorsiflexed

(continued)

Table 2. (continued)

Study	Patients	Study Objectives	Methods	Findings
Ledoux et al, 2006 ¹⁹	<ul style="list-style-type: none"> • 10 healthy controls • 10 patients with pes cavus deformity • 10 patients with asymptomatic pes planus deformity • 10 patients with symptomatic pes planus deformity 	Differences in bone-to-bone relationships between different foot types	Special frame with 20% of weightbearing in supine position	Significant differences were found in all measurements regarding midfoot and hindfoot alignment
Malicky et al, 2002 ²⁴	<ul style="list-style-type: none"> • 5 healthy controls • 19 patients with symptomatic flatfoot deformity with lateral pain 	Osseous relationships in patients with flatfoot deformity and to evaluate subfibular impingement	75-N axial force with a custom loading frame in supine position	<ul style="list-style-type: none"> • Prevalence of sinus tarsi impingement 92% vs 0% in controls • Prevalence of calcaneofibular impingement 66% vs 5% in controls
Van Bergeyk et al, 2002 ³⁰	<ul style="list-style-type: none"> • 12 healthy controls • 11 patients with chronic lateral instability 	Radiographic differences with respect to hindfoot varus/valgus between patients with chronic lateral instability and controls	Special frame with full weightbearing in supine position	Hindfoot alignment angle was different in both groups: 6.4 ± 4 degrees varus (patients with instability) vs 2.7 ± 5 degrees varus (controls)
Yoshioka et al, 2016 ³¹	<ul style="list-style-type: none"> • 10 healthy controls • 10 patients with stage II PTTD flatfoot deformity 	Forefoot and hindfoot alignment	Special frame with full weightbearing in supine position	<ul style="list-style-type: none"> • Meary's angle was significantly lower in flatfeet • First metatarsal more everted in flatfeet • Calcaneus was more everted and abducted in flatfeet
Zhang et al, 2013 ³²	<ul style="list-style-type: none"> • 15 healthy controls • 15 patients with stage II PTTD flatfoot deformity 	Rotation and translation of hindfoot joints	Special frame with full weightbearing in supine position	Significant differences in position of talus, navicular, and calcaneus between both groups

Abbreviations: HV, hallux valgus; PTT, posterior tibial tendon; PTTD, posterior tibial tendon dysfunction; 3D, 3-dimensional; TMT, tarsometatarsal; TN, talonavicular.

foot pain ($n = 5$), and others ($n = 3$). Significant differences were found for all measurements except the hindfoot alignment angle and tibio-calcaneal distance when comparing weightbearing and nonweightbearing images. These included differences in fibulocalcaneal distance, lateral talocalcaneal joint space, talocalcaneal overlap, and naviculocalcaneal distance.¹² The hindfoot alignment angle was comparable when measured with and without weightbearing (21.0 ± 7.9 degrees vs 19.0 ± 9.0 degrees).¹² These findings suggest that radiographic assessment of impingement (eg, using fibulocalcaneal distance) should be performed using weightbearing conditions.

Kim et al¹⁶ used semi-WtBCT to assess the preoperative forefoot alignment in 138 patients (166 feet) with hallux valgus deformities and compared the results to a control group with 19 patients (19 feet). In all persons, the α angle (first metatarsal pronation angle) was measured to assess

the forefoot alignment in the coronal view. Furthermore, the sesamoid position was evaluated using a 4-stage grading system by Smith et al.²⁸ The α angle was significantly different between the hallux valgus and control groups (21.9 degrees and 13.8 degrees, respectively). Four different classification groups of hallux valgus deformity were developed based on first metatarsal pronation and sesamoid subluxation, leading the authors to suggest that the use of semi-WtBCT may be helpful to assess the forefoot deformity in the coronal plane and guide treatment choice.²⁸

Richter et al²⁷ recently published 2 studies examining WtBCT. In the first study, 30 consecutive patients were prospectively enrolled to assess forefoot and hindfoot alignment using WtBCT (Figures 1 and 2), CT without weightbearing, and conventional weightbearing radiographs.²⁶ Significant differences were found in measured angles between imaging modalities (Table 4).²⁶ For

Table 3. Description of 8 Studies Included in the Systematic Literature Review.

Study	Study Type	Data Collection	Level of Evidence	Conflict of Interest	Patients
Burssens et al, 2016 ³	Multicenter	Retrospective	III	None	<ul style="list-style-type: none"> 60 patients (30 valgus and 30 varus malalignment)
Cody et al, 2016 ⁵	Single center	Retrospective	III	None	<ul style="list-style-type: none"> 45 patients with adult-acquired flatfoot deformity 17 healthy controls
Collan et al, 2013 ⁷	Single center	Prospective	II	None	<ul style="list-style-type: none"> 10 patients with bilateral hallux valgus deformity 5 healthy controls
Hirschmann et al, 2014 ¹²	Single center	Prospective	IV	NR	<ul style="list-style-type: none"> 22 patients with different hindfoot pathologies
Krähenbühl et al, 2016 ¹⁸	Single center	Retrospective	III	None	<ul style="list-style-type: none"> 40 patients with subtalar osteoarthritis 20 healthy controls
Lintz et al, 2017 ²³	Multicenter	Retrospective	III	Yes ^a	<ul style="list-style-type: none"> 135 patients: normal (57), varus (38), and valgus (40) alignment
Richter et al, 2014 ²⁶	Single center	Prospective	IV	Yes ^b	<ul style="list-style-type: none"> 30 patients with foot/ankle disorders
Richter et al, 2015 ²⁷	Single center	Prospective	IV	Yes ^b	<ul style="list-style-type: none"> First study: 30 patients Second study: 50 patients

Abbreviation: NR, not reported.

^aThe corresponding author received personal fees from Curvebeam during the conduct of the study.

^bThe corresponding author is a consultant of Stryker, Intercus, and Curvebeam; proprietor of R-innovation; and joint proprietor of first Worldwide Orthopaedics.

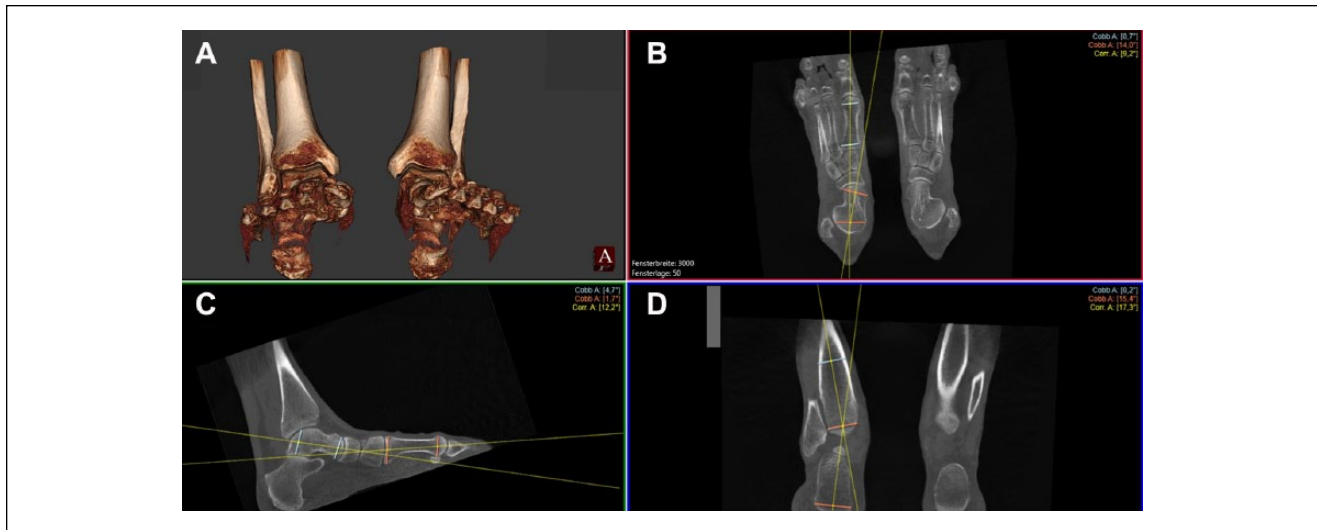


Figure 1. PedCAT angle measurements. (A) The 3-dimensional (3D) reformation demonstrates how the 3D data set was virtually rotated to allow for exact congruency of the plane of the reformations with the bone axes as described before.^{26,27} Measurement of the dorsoplantar tarsometatarsal angle in the (B) horizontal plane and in the (C) sagittal plane. (D) Hindfoot alignment measurement. The lines that define the centers of the bones proximally and distally are exactly 50% of the measured bone thickness distance.

instance, hindfoot alignment angle on WtBCT was 10.1 ± 7.1 degrees while 5.4 ± 5.6 degrees on conventional CT and 2.4 ± 6.9 degrees on weightbearing radiographs. The second study was a prospective consecutive study of 50 patients who underwent WtBCT and simultaneous pedobarography.²⁷ The pedobarography consisted of the

following computerized mapping: hindfoot, midfoot, first metatarsal head/sesamoids area, second metatarsal head, third metatarsal head, fourth metatarsal head, fifth metatarsal head, first toe, second toe, and third to fifth toes. No substantial correlation was found between WtBCT measurements and pedobarography values, leading the authors

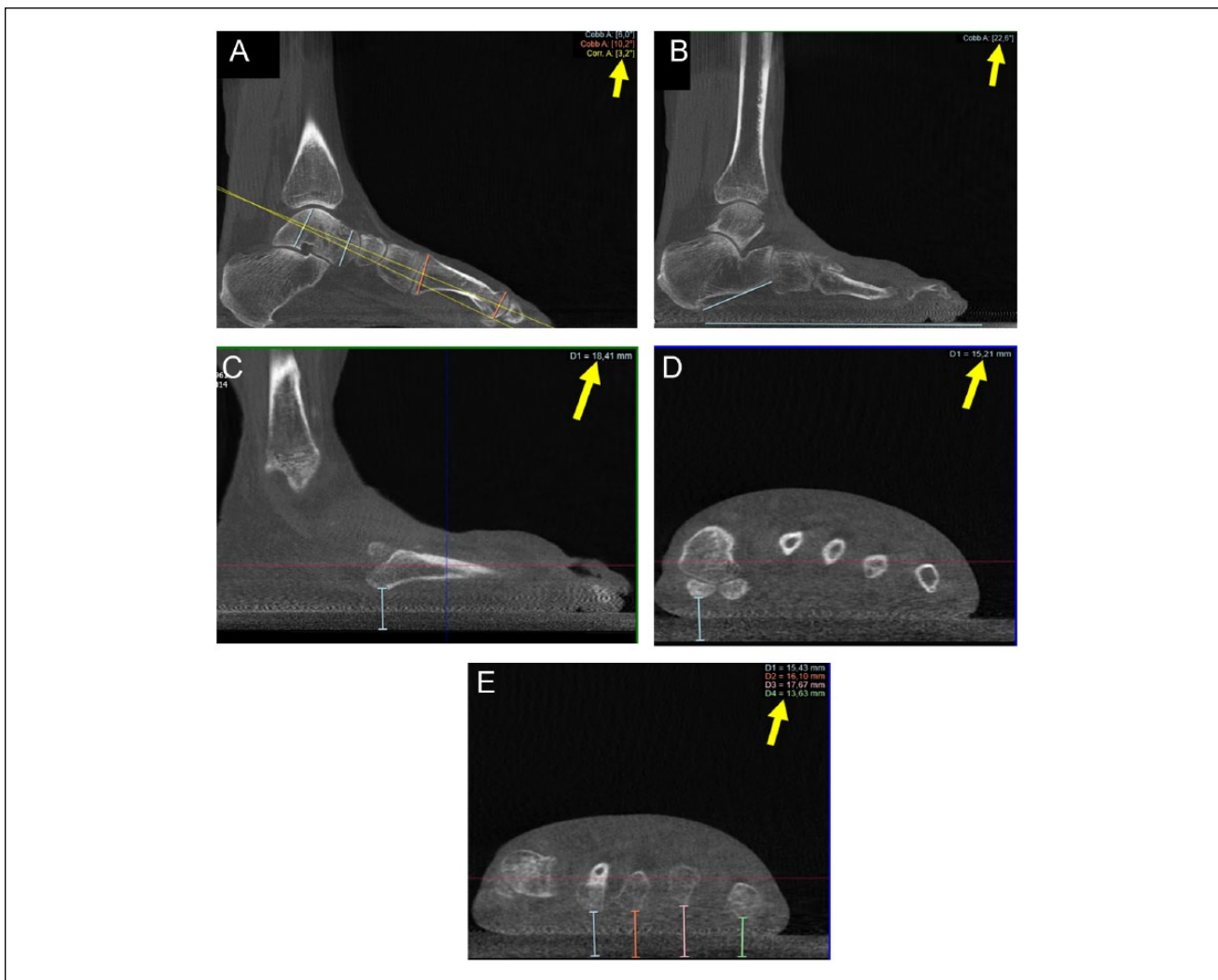


Figure 2. PedCAT angle and distance measurements. (A) Lateral tarsometatarsal angle in the sagittal plane (here 3.2°). (B) Calcaneal pitch angle in the sagittal plane (here 22.6°). (C) Minimum distance between fifth metatarsal bone to footplate in the sagittal plane (here 18 mm). (D) Height of medial sesamoid in the coronal plane (here 15 mm). (E) Height of second to fifth metatarsal heads in the coronal plane (here 15, 16, 18, and 14 mm, respectively).

to conclude that WtBCT is not useful in assessing plantar force and pressure distributions.²⁷

Burssens et al³ recently described a clinically relevant and reproducible method to measure hindfoot alignment using WtBCT. Sixty patients were enrolled into this prospective study, including 2 groups: 30 patients with varus alignment and 30 patients with valgus alignment. Hindfoot alignment was measured using 3 different angles (Figure 3): by the bisector of the Achilles tendon and the calcaneus (HAA_{CL}), by standard method using an inclination set at 45 degrees (to simulate the long axial view) (HAA_{LA}), and by a novel method that combines the inclination of the tibia (anatomical axis) and inclination of the talus and calcaneus (talocalcaneal angle) (HAA_{NOV}). The novel hindfoot angle assessment demonstrated a positive correlation with previous hindfoot angles, a high correlation with

clinical alignment assessment, and an excellent reliability. The authors concluded that WtBCT can be used to objectively measure hindfoot alignment similar to plain films.³

Cody et al⁵ used WtBCT to analyze the talar anatomy and subtalar joint alignment in patients with adult-acquired flatfoot deformity. In total, 45 patients with stage II flatfoot deformity and 17 control patients were enrolled into this study. The subtalar joint alignment was assessed using 2 angles: (1) angle between the inferior facet of the talus and the horizontal line and (2) angle between the inferior and superior facets of the talus. Both angles were significantly different in both groups. Specifically, it was demonstrated that patients with flatfoot deformity had more innate valgus in their talar anatomy and more valgus alignment of the subtalar joint. This information might potentially be used to identify patients who have a higher risk for underlying deformity progression.⁵

Table 4. Radiographic Assessment of the Forefoot Using Weightbearing Computed Tomography.

Radiographic Measurement	Interobserver Reliability	Intraobserver Reliability	Correlation With Other Measurements	Clinical Findings
α angle (first MT pronation angle)	NA	NA	<ul style="list-style-type: none"> vs HVA¹⁶: .076,^a $P < .1$ vs IMA¹⁶: .144,^a $P < .1$ vs sesamoid position¹⁶: .019,^a $P < .1$ 	<ul style="list-style-type: none"> HV group: 21.9 degrees, control group: 13.8 degrees¹⁶ HV group: 8 \pm 2 degrees (4-12 degrees), control group: 2 \pm 3 degrees (-4 to 8 degrees)⁷
First MT/ground angle	NA	NA	NA	<ul style="list-style-type: none"> HV group: 18 \pm 1 degrees, control group: 21 \pm 1 degrees⁷
HVA (2D)	NA	NA	NA	<ul style="list-style-type: none"> HV group: 35 \pm 3 degrees, control group: 13 \pm 4 degrees⁷
HVA (3D)	NA	NA	<ul style="list-style-type: none"> vs HVA on plain radiographs⁷: .95,^b $P < .05$ vs HVA (2D)⁷: .94,^b $P < .05$ 	<ul style="list-style-type: none"> HV group: 35 \pm 3 degrees (WB), 46 \pm 5 degrees (NWB), control group: 15 \pm 4 degrees (WB), 32 \pm 8 degrees (NWB)⁷
IMA (2D)	NA	NA	NA	<ul style="list-style-type: none"> HV group: 19 \pm 1 degrees, control group: 11 \pm 1 degrees⁷
IMA (3D)	NA	NA	<ul style="list-style-type: none"> vs IMA on plain radiographs⁷: .72,^b $P < .05$ vs IMA (2D)⁷: .81,^b $P < .05$ 	<ul style="list-style-type: none"> HV group: 17 \pm 1 degrees (WB), 14 \pm 1 degrees (NWB), control group: 11 \pm 1 degrees (WB), 8 \pm 2 degrees (NWB)⁷ 9.3 \pm 3.5 degrees (WB), 7.8 \pm 3.9 degrees (NWB)²⁷
Maximum horizontal width (mm)	NA	NA	NA	<ul style="list-style-type: none"> HV group: 98 \pm 1 degrees (WB), 89 \pm 2 degrees (NWB), control group: 86 \pm 2 degrees (WB), 78 \pm 3 degrees (NWB)⁷
Sesamoid position in coronal plane	NA	NA	<ul style="list-style-type: none"> vs α angle¹⁶: .019,^a $P < .1$ vs HVA¹⁶: .477,^a $P < .01$ 	<ul style="list-style-type: none"> HV group: true sesamoid subluxation 71.7%, no sesamoid subluxation 28.3%¹⁶
TMT angle dorsoplantar	NA	NA	NA	<ul style="list-style-type: none"> -5.0 \pm 12.0 degrees (WB), 4.3 \pm 10.0 degrees (NWB)²⁷
TMT angle lateral	NA	NA	NA	<ul style="list-style-type: none"> -7.6 \pm 8.2 degrees (WB), 0.5 \pm 8.4 (NWB)²⁷

Abbreviations: HV, hallux valgus; HVA, hallux valgus angle; IMA, intermetatarsal angle; MT, metatarsal; NA, not available; NWB, nonweightbearing; 2D, 2-dimensional; 3D, 3-dimensional; TMT, tarsometatarsal; WB, weightbearing.

^aSpearman rank correlation coefficient.

^bPearson correlation coefficient.

Krähenbühl et al¹⁸ analyzed the orientation of the subtalar joint in 40 patients with tibiotalar osteoarthritis and 20 healthy controls. The subtalar joint was assessed by measurement of the subtalar vertical angle using WtBCT. Comparison of the varus and valgus joint between healthy controls and affected joints revealed significant differences in the subtalar vertical angle measurements. The findings of this study suggest that the orientation of the subtalar joint may be an important factor in the development of ankle joint osteoarthritis.¹⁸

Lintz et al²³ described a new 3D biometric tool for hindfoot alignment assessment using WtBCT. Data sets from 135 patients were analyzed: 57 with normal hindfoot alignment, 38 with varus hindfoot alignment, and 40 with valgus hindfoot alignment. Foot and ankle offset represents the lever arm of the torque generated in the ankle from the combined actions of body weight and ground reaction force. In patients

with neutral hindfoot alignment, the offset was 2.3% \pm 2.9%. In patients with varus and valgus alignment, the offset was -11.6% \pm 6.9% and 11.4% \pm 5.7%, respectively. The findings of this pilot study suggest that the measurement of the foot and ankle offset can be used as a tool for hindfoot alignment assessment. However, further clinical studies should highlight its importance and relevance in clinical use. Furthermore, it needs to be addressed whether WtBCT is superior to plain films with regard to assessment of hindfoot alignment.²³

Radiographic Measurements Using Weightbearing CT

In the available literature, several measurements have been described to assess the forefoot alignment (Table 4) and mid-foot/hindfoot alignment (Table 5) using WtBCT (Figure 4). The forefoot measurements include specifically assessment

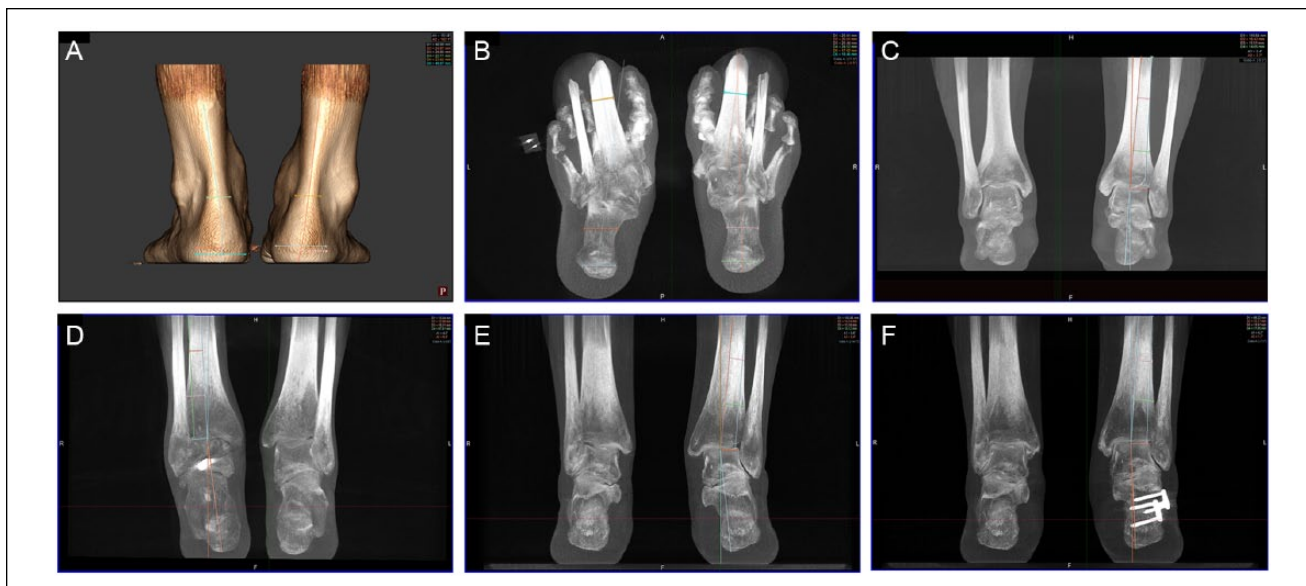


Figure 3. Hindfoot alignment measurements in weightbearing computed tomography. (A) HAA_{CL} : according to the clinical position by the intersection of the bisecting axis through the Achilles tendon and calcaneal surfaces measured in the posteroanterior view. (B) HAA_{LA} : hindfoot alignment measured using a simulated long axial view. (C) HAA_{NOV} : determined by combination of the tibia inclination (anatomical tibial axis, middle line through the proximal and tibial tibia) and inclination of the talus and calcaneus (talocalcaneal axis connecting the inferior calcaneus point and the middle of the talar dome) in a person with neutral alignment in the anteroposterior view. (D) HAA_{NOV} in a patient with varus alignment. (E) HAA_{NOV} in a patient with valgus alignment. (F) HAA_{NOV} in a patient following operative correction of valgus alignment.

Table 5. Radiographic Assessment of the Midfoot and Hindfoot Using Weightbearing Computed Tomography.

Radiographic Measurement	Interobserver Reliability	Intraobserver Reliability	Correlation With Other Measurements	Clinical Findings
Calcaneal pitch angle	NA	NA	NA	• 17.8 ± 5.4 degrees (WB), 16.5 ± 5.0 degrees (NWB) ²⁷
Calcaneofibular distance (mm)	$0.61^{a,12}$	NA	NA	• 0.3 ± 6.0 (WB), 3.6 ± 5.2 (NWB) ¹²
Foot and ankle offset (%)	$0.99 \pm 0.00^{b,23}$	0.97 ± 0.02	NA	• 2.3 ± 2.9 (95% CI, 1.5-3.1) (patients with neutral alignment) ²³ • -11.6 ± 6.9 (95% CI, -13.9 to -9.4) (patients with varus alignment) ²³ • 11.4 ± 5.7 (95% CI, 9.6-13.3) (patients with valgus alignment) ²³
HAA	$0.83^{a,12}$	NA	NA	• 21.0 ± 7.9 degrees (WB), 19.0 ± 9.0 degrees (NWB) ¹² • 10.1 ± 7.1 degrees (WB), 5.4 ± 5.6 degrees (NWB) ²⁷
HAA_{CL}	0.72 (valgus), 0.69 (varus) ^{b,3}	0.73 (valgus), 0.67 (varus) ³	NA	• 25.2 degrees (valgus), 22 degrees (varus) ³
HAA_{LA}	0.7 (valgus), 0.71 (varus) ^{b,3}	0.71 (valgus), 0.72 (varus) ³	NA	• 16.4 degrees (valgus), 11.9 degrees (varus) ³
HAA_{NOV}	0.69 (valgus), 0.6 (varus) ^{b,3}	0.67 (valgus), 0.67 (varus) ³	NA	• 17.7 degrees (valgus), 13.5 degrees (varus) ³
Lateral talocalcaneal joint space width (mm)	$0.82^{a,12}$	NA	NA	• 2.2 ± 1.1 (WB), 2.9 ± 1.7 (NWB) ¹²
Naviculocalcaneal distance (mm)	$0.85^{a,12}$	NA	NA	• 15.3 ± 4.7 (WB), 13.5 ± 4.0 (NWB) ¹²

(continued)

Table 5. (continued)

Radiographic Measurement	Interobserver Reliability	Intraobserver Reliability	Correlation With Other Measurements	Clinical Findings
Subtalar inferior facet–horizontal angle	NA	NA	<ul style="list-style-type: none"> No correlation with any weightbearing radiographic measures⁵ 	<ul style="list-style-type: none"> Stage II AAFD group: 15.9 ± 5.7 degrees, control group: 5.7 ± 6.7 degrees⁵
Subtalar inferior–superior facets angle	NA	NA	<ul style="list-style-type: none"> vs AP coverage angle⁵: $P = .003$ vs AP talar-first MT angle: $P = .003$ vs calcaneal pitch⁵: $P = .014$ vs Meary's angle⁵: $P < .001$ vs medial column height⁵: $P = .007$ 	<ul style="list-style-type: none"> Stage II AAFD group: 21.2 ± 6.7 degrees, control group: 10.7 ± 6.4 degrees⁵
Subtalar vertical angle	<ul style="list-style-type: none"> 0.975^{a,18} 0.72 (valgus), 0.73 (varus)^{b,3} 	<ul style="list-style-type: none"> 0.989¹⁸ 0.77 (valgus), 0.78 (varus)³ 	NA	<ul style="list-style-type: none"> 91 degrees (72-109 degrees) (varus OA group), 109 degrees (97-120 degrees) (valgus OA group), 98 degrees (85-114 degrees) (controls)¹⁸ 74.3 degrees (valgus), 69.1 degrees (varus)³
Talar tilt	0.92 (valgus), 0.89 (varus) ^{b,3}	0.89 (valgus), 0.89 (varus) ³	NA	<ul style="list-style-type: none"> 5.9 degrees (valgus), 4.8 degrees (varus)³
Talar translation (mm)	0.86 (valgus), 0.82 (varus) ^{b,3}	0.87 (valgus), 0.88 (varus) ³	NA	<ul style="list-style-type: none"> 21 degrees (valgus), 19 degrees (varus)³
Talocalcaneal overlap (mm)	0.81 ^{c,12}	NA	NA	<ul style="list-style-type: none"> 1.4 ± 3.9 degrees (WB), 4.1 ± 3.9 degrees (NWB)¹²
Tibiocalcaneal distance (mm)	0.72 ^{c,12}	NA	NA	<ul style="list-style-type: none"> 20.6 ± 4.2 degrees (WB), 21.7 ± 6.2 degrees (NWB)¹²

Abbreviations: AAFD, adult-acquired flatfoot deformity; AP, anteroposterior; CI, confidence interval; HAA, hindfoot alignment angle; HAA_{CL}, hindfoot alignment angle measured by the bisector of the Achilles tendon and the calcaneus⁵; HAA_{LA}, hindfoot alignment angle measured using an inclination set at 45 degrees to simulate the long axial view³; HAA_{NOV}, hindfoot alignment angle measured by combining the inclination of the tibia (anatomical axis) and inclination of the talus and calcaneus (talocalcaneal angle)³; MT, metatarsal; NA, not available; OA, osteoarthritis; NWB, nonweightbearing; WB, weightbearing.

^aIntraclass correlation coefficient to assess the interobserver reliability (measurements of 1 orthopaedic resident, 1 medical student, and 1 scientific associate).

^bIntraclass correlation coefficient to assess the interobserver reliability (measurement of 2 independent observers).

^cIntraclass correlation coefficient to assess the interobserver reliability (measurements of 2 musculoskeletal radiologists).

of hallux valgus deformity (α angle, hallux valgus angle, intermetatarsal angle, and tarsometatarsal angle). The hindfoot measurements include foot and ankle offset, hindfoot alignment angle, and osseous relationship (eg, talocalcaneal overlap and tibiocalcaneal distance).

Future Directions

Standardization of Measurements Using WtBCT

First, all forefoot, midfoot, and hindfoot alignment measurements using WtBCT should be standardized by reliable identification of anatomic landmarks. All measurements should then be performed in healthy asymptomatic persons to identify the normal values. Furthermore, the intraobserver and interobserver reliability for all measurements at different training levels, including research associate, medical student, orthopaedic resident, orthopaedic foot and ankle surgeon, and musculoskeletal radiologist, should be assessed. Finally, clinical studies should clarify whether forefoot, midfoot, and hindfoot measurements using WtBCT are clinically relevant and superior to using plain films.

WtBCT vs Plain Films

All forefoot, midfoot, and hindfoot alignment measurements using WtBCT should be correlated with those using conventional weightbearing radiographs. It still remains unclear whether weightbearing has a substantial influence on alignment measurements. WtBCT offers the possibility to use digitally reconstructed radiographs, but those radiographs should be correlated with conventional plain films.

Conclusions

The use of WtBCT has steadily increased over the past 5 years. WtBCT has been shown to offer several advantages, including imaging in the physiological standing position, high spatial resolution, fast imaging acquisition time, low radiation dose, and modest costs. Cone-beam CT technology with current design and flexible gantry movements allows both supine and standing weightbearing imaging of the lower extremity with comparable quality but lower radiation than with conventional CT scanning. WtBCT can be used to investigate the normal anatomy and dynamics (eg, rotational

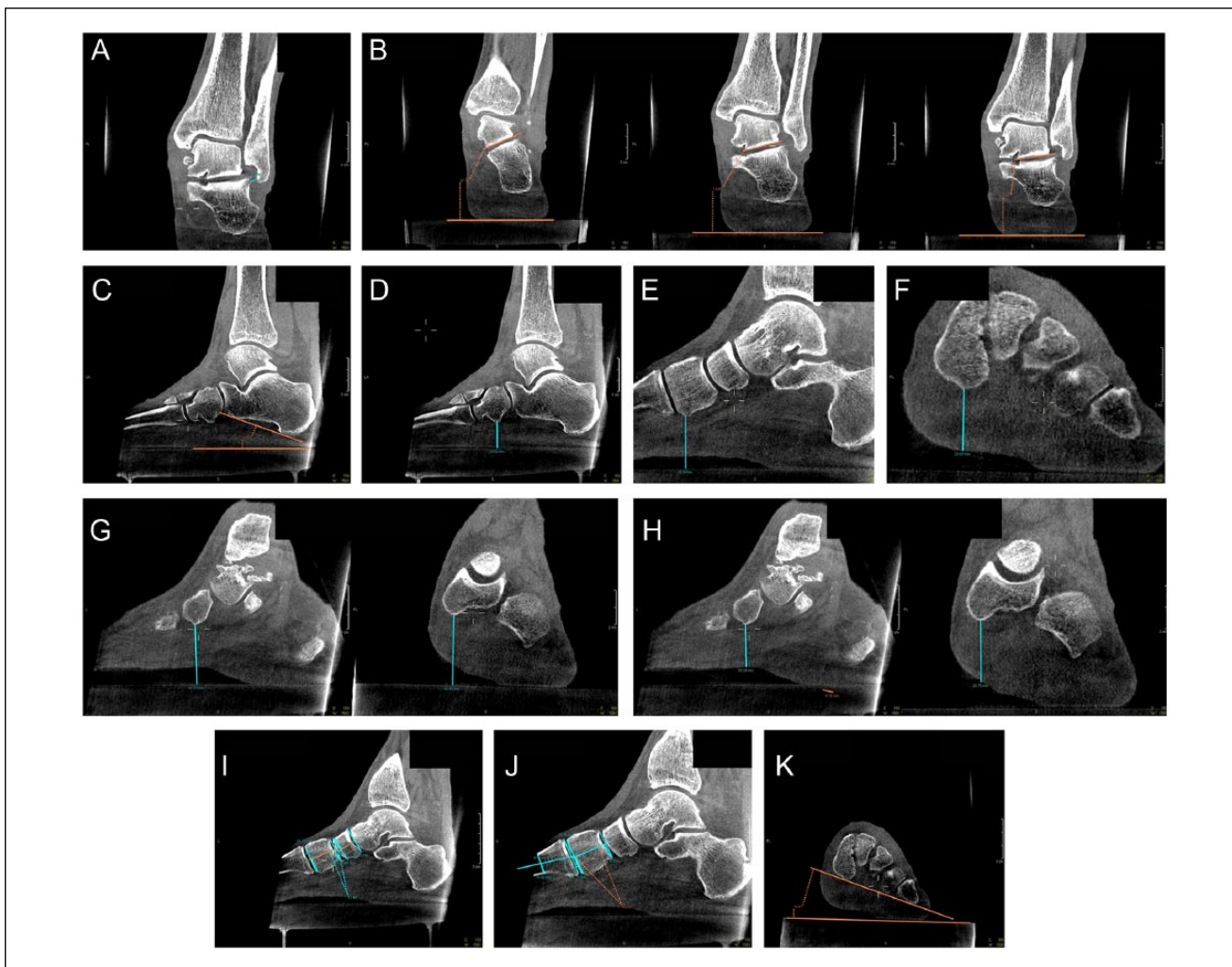


Figure 4. Hindfoot, midfoot, and forefoot alignment measurements using weightbearing computed tomography. (A) Calcaneofibular distance in the coronal plane. (B) Subtalar horizontal angle in the coronal plane. (C) Calcaneal inclination angle in the sagittal plane. (D) Cuboid-floor distance in the sagittal plane. (E) Cuneiform-floor distance in the sagittal plane. (F) Cuneiform-skin distance in the coronal plane. (G) Navicular-floor distance in the sagittal and coronal planes. (H) Navicular-skin distance in the sagittal and coronal planes. (I) Navicular-cuneiform angle in the sagittal plane. (J) Cuneiform-first metatarsal angle in the sagittal plane. (K) Forefoot arch angle in the coronal plane.

dynamics) of the hindfoot.^{20,21} In the clinic, WtBCT can be used to assess forefoot and hindfoot alignment. Further work needs to be done to validate and standardize measurement approaches that will facilitate communication between investigators and clinicians on the nature and treatment of foot and ankle deformities.

Acknowledgment

We thank Maxwell Weinberg, MS (Department of Orthopaedics, University of Utah, Salt Lake City, UT) for his help with manuscript correction and editing review.

Declaration of Conflicting Interests

The author(s) declared the following potential conflicts of interest with respect to the research, authorship, and/or publication of this

article: Martinus Richter, MD, PhD, François Lintz, MD, FEBOT, and Arne Burssens, MD, report personal fees from Curvebeam LLC outside the submitted work. ICMJE forms for all authors are available online.

Funding

The author(s) received no financial support for the research, authorship, and/or publication of this article.

References

1. Ananthakrisnan D, Ching R, Tencer A, Hansen ST Jr, Sangeorzan BJ. Subluxation of the talocalcaneal joint in adults who have symptomatic flatfoot. *J Bone Joint Surg Am.* 1999;81(8):1147-1154.
2. Apostle KL, Coleman NW, Sangeorzan BJ. Subtalar joint axis in patients with symptomatic peritalar subluxation

- compared to normal controls. *Foot Ankle Int.* 2014;35(11):1153-1158.
3. Burssens A, Peeters J, Buedts K, Victor J, Vandeputte G. Measuring hindfoot alignment in weight bearing CT: a novel clinical relevant measurement method. *Foot Ankle Surg.* 2016;22(4):233-238.
 4. Carrino JA, Al Muhit A, Zbujewski W, et al. Dedicated cone-beam CT system for extremity imaging. *Radiology.* 2014;270(3):816-824.
 5. Cody EA, Williamson ER, Burket JC, Deland JT, Ellis SJ. Correlation of talar anatomy and subtalar joint alignment on weightbearing computed tomography with radiographic flat-foot parameters. *Foot Ankle Int.* 2016;37(8):874-881.
 6. Colin F, Horn Lang T, Zwicky L, Hintermann B, Knupp M. Subtalar joint configuration on weightbearing CT scan. *Foot Ankle Int.* 2014;35(10):1057-1062.
 7. Collan L, Kankare JA, Mattila K. The biomechanics of the first metatarsal bone in hallux valgus: a preliminary study utilizing a weight bearing extremity CT. *Foot Ankle Surg.* 2013;19(3):155-161.
 8. Di Giulio I, Maganaris CN, Baltzopoulos V, Loram ID. The proprioceptive and agonist roles of gastrocnemius, soleus and tibialis anterior muscles in maintaining human upright posture. *J Physiol.* 2009;587(pt 10):2399-2416.
 9. Ferri M, Scharfenberger AV, Goplen G, Daniels TR, Pearce D. Weightbearing CT scan of severe flexible pes planus deformities. *Foot Ankle Int.* 2008;29(2):199-204.
 10. Geng X, Wang C, Ma X, et al. Mobility of the first metatarsal-cuneiform joint in patients with and without hallux valgus: in vivo three-dimensional analysis using computerized tomography scan. *J Orthop Surg Res.* 2015;10:140.
 11. Greisberg J, Hansen ST Jr, Sangeorzan B. Deformity and degeneration in the hindfoot and midfoot joints of the adult acquired flatfoot. *Foot Ankle Int.* 2003;24(7):530-534.
 12. Hirschmann A, Pfirrmann CW, Klammer G, Espinosa N, Buck FM. Upright cone CT of the hindfoot: comparison of the non-weight-bearing with the upright weight-bearing position. *Eur Radiol.* 2014;24(3):553-558.
 13. Katsui R, Samoto N, Taniguchi A, et al. Relationship between displacement and degenerative changes of the sesamoids in hallux valgus. *Foot Ankle Int.* 2016;37(12):1303-1309.
 14. Kido M, Ikoma K, Imai K, et al. Load response of the tarsal bones in patients with flatfoot deformity: in vivo 3D study. *Foot Ankle Int.* 2011;32(11):1017-1022.
 15. Kido M, Ikoma K, Imai K, et al. Load response of the medial longitudinal arch in patients with flatfoot deformity: in vivo 3D study. *Clin Biomech (Bristol, Avon).* 2013;28(5):568-573.
 16. Kim Y, Kim JS, Young KW, et al. A new measure of tibial sesamoid position in hallux valgus in relation to the coronal rotation of the first metatarsal in CT scans. *Foot Ankle Int.* 2015;36(8):944-952.
 17. Kimura T, Kubota M, Taguchi T, et al. Evaluation of first-ray mobility in patients with hallux valgus using weight-bearing CT and a 3-D analysis system: a comparison with normal feet. *J Bone Joint Surg Am.* 2017;99(3):247-255.
 18. Krähenbühl N, Tschuck M, Bolliger L, Hintermann B, Knupp M. Orientation of the subtalar joint: measurement and reliability using weightbearing CT scans. *Foot Ankle Int.* 2016;37(1):109-114.
 19. Ledoux WR, Rohr ES, Ching RP, Sangeorzan BJ. Effect of foot shape on the three-dimensional position of foot bones. *J Orthop Res.* 2006;24(12):2176-2186.
 20. Lepojärvi S, Niinimäki J, Pakarinen H, Koskela L, Leskela HV. Rotational dynamics of the talus in a normal tibiotalar joint as shown by weight-bearing computed tomography. *J Bone Joint Surg Am.* 2016;98(7):568-575.
 21. Lepojärvi S, Niinimäki J, Pakarinen H, Leskela HV. Rotational dynamics of the normal distal tibiofibular joint with weight-bearing computed tomography. *Foot Ankle Int.* 2016;37(6):627-635.
 22. Linklater JM, Read JW, Hayter CL. Imaging of the foot and ankle. In: Coughlin MJ, Saltzman CL, Anderson RB, eds. *Mann's Surgery of the Foot and Ankle.* 9th ed. Philadelphia, PA: Elsevier Saunders; 2014:61-120.
 23. Lintz F, Welck M, Bernasconi A, et al. 3D biometrics for hindfoot alignment using weightbearing CT. *Foot Ankle Int.* 2017;38(6):684-689.
 24. Malicky ES, Crary JL, Houghton MJ, et al. Talocalcaneal and subfibular impingement in symptomatic flatfoot in adults. *J Bone Joint Surg Am.* 2002;84(11):2005-2009.
 25. Mettler FA Jr, Huda W, Yoshizumi TT, Mahesh M. Effective doses in radiology and diagnostic nuclear medicine: a catalog. *Radiology.* 2008;248(1):254-263.
 26. Richter M, Seidl B, Zech S, Hahn S. PedCAT for 3D-imaging in standing position allows for more accurate bone position (angle) measurement than radiographs or CT. *Foot Ankle Surg.* 2014;20(3):201-207.
 27. Richter M, Zech S, Hahn S. PedCAT for radiographic 3D-imaging in standing position. *Fuss Sprungg.* 2015;13(2): 85-102.
 28. Smith RW, Reynolds JC, Stewart MJ. Hallux valgus assessment: report of research committee of American Orthopaedic Foot & Ankle Society. *Foot Ankle.* 1984;5(2): 92-103.
 29. Tuominen EK, Kankare J, Koskinen SK, Mattila KT. Weight-bearing CT imaging of the lower extremity. *AJR Am J Roentgenol.* 2013;200(1):146-148.
 30. Van Bergeyk AB, Younger A, Carson B. CT analysis of hind-foot alignment in chronic lateral ankle instability. *Foot Ankle Int.* 2002;23(1):37-42.
 31. Yoshioka N, Ikoma K, Kido M, et al. Weight-bearing three-dimensional computed tomography analysis of the forefoot in patients with flatfoot deformity. *J Orthop Sci.* 2016;21(2):154-158.
 32. Zhang Y, Xu J, Wang X, et al. An in vivo study of hindfoot 3D kinetics in stage II posterior tibial tendon dysfunction (PTTD) flatfoot based on weight-bearing CT scan. *Bone Joint Res.* 2013;2(12):255-263.